Journal of Molecular Catalysis A: Chemical 301 (2009) 118–126

Contents lists available at ScienceDirect

Journal of Molecular Catalysis A: Chemical

journal homepage: www.elsevier.com/locate/molcata

Catalytic Meerwein-Ponndorf-Verley reductions over mesoporous silica supports: Rational design of hydrophobic mesoporous silica for enhanced stability of aluminum doped mesoporous catalysts

S. Shylesh[a,*], Mahendra P. Kapoor[b], Lekh. R. Juneja[b], Prinson P. Samuel[a], Ch. Srilakshmi[c], A.P. Singh[a,*]

[a] Inorganic and Catalysis Division, National Chemical Laboratory, Pune 411008, India
[b] NanoFunction Division, Taiyo Kagaku Co. Ltd., 1-3 Takaramachi, Yokkaichi, Mie 510-0884, Japan
[c] Institute of Chemical and Engineering Sciences, Jurong Island, Singapore 627883, Singapore

ARTICLE INFO

Article history:
Received 22 September 2008
Received in revised form 17 November 2008
Accepted 19 November 2008
Available online 27 November 2008

Keywords:
Mesoporous silica
Organosilica
Aluminum isopropoxide
Reduction

ABSTRACT

A series of aluminum isopropoxide-grafted mesoporous organosilica having ethane (–CH_2–CH_2–) and ethene (–CH=CH–) groups in the frame wall positions (ethane–silica, ethene–silica) as well as mesoporous silicas (MCM-41, MCM-48, SBA-15) through siloxide linkages were fabricated. The samples were used as catalysts in the Meerwein-Ponndorf-Verley reduction of ketones and aldehydes of different nature and size using secondary alcohols as the hydrogen transfer agents. Aluminum isopropoxide supported mesoporous silica samples show higher catalytic conversion and among them, the one-dimensionally channel oriented Si-MCM-41 supported aluminum isopropoxide shows better results than the three-dimensional Si-MCM-48 and the large pore Si-SBA-15. Compared to aluminum isopropoxide-grafted mesoporous silica samples, aluminum alkoxide-grafted organosilica samples shows better catalytic activity even in the presence of 10% of water and the better stability is attributed to the presence of integrated hydrophobic organic groups in the frame wall positions.

1. Introduction

The Meerwein-Ponndorf-Verley (MPV) reduction of carbonyl compounds to primary and secondary alcohols involves equilibrium driven, reversible hydride transfer from a secondary alcohol, to a carbonyl substrate *via* a six-membered transition state, initiated by the activation of the carbonyl groups by coordination to the Lewis acidic aluminum centre [1–3]. The classical MPV reduction reaction is carried out in the presence of aluminum alkoxides like $Al(O^iPr)_3$ and ^{i}PrOH hydride source which offers many practical advantages like the mild reaction conditions, safe and simple operations and chemo selective nature—that unsaturated aldehydes and ketones are not reduced to saturated alcohols. However, the usage of stoichiometric amount of aluminum alkoxides, need for excess alcohols, low reaction rate due to the poor reactivity of traditional aluminum catalyst, as well as the formation of condensed products limits its wide applicability [4,5]. Hence, a high reaction temperature with the concurrent removal of the byproduct acetone from the system was applied so as to shift the equilibrium towards the formation of alcohols; but these in turn enhance side reactions like aldol condensation or the Tishchenko reactions [6].

Because of these reasons, a variety of aluminum catalysts are employed for the MPV reduction reactions. Simple alkyl aluminum reagents like $AlMe_3$ or $AlEt_3$ had shown very high activity in the MPV reductions and the high activity is attributed to the *in situ* formation of aluminum alkoxide species in the presence of excess isopropanol [7]. These results indeed show that elaborate ligands are not needed for obtaining high activity and selectivity in reduction reactions. Ooi et al. used a bidentate aluminum catalyst for the reduction process and had shown the reduction of a wide range of ketones and aldehydes in good yields [8]. Various other metal alkoxides, like the lanthanum alkoxides, are also used as catalysts for the reduction of carbonyl compounds [9,10]. However, many of these catalysts are homogenous and because of the difficulties associated with separating the products from the catalyst and from any reaction solvent urged for stable, recyclable solid catalysts. VanBekkum and colleagues found that zeolite beta catalyze the reduction of 4-*tert*-butyl cyclohexanone with a high stereo selectivity to the *cis*-isomer and had shown that Lewis acid sites are the active catalytic sites [11–15]. Subsequently, numerous metal oxides with acidic as well as basic properties are also found active in the reduction process [16–19]. Very recently, Corma et al. had shown that Sn-Beta and Zhu et al. had shown that Zr-beta and zirconium propoxide-grafted SBA-15 samples are efficient catalysts for the MPV reduction

* Corresponding authors. Tel.: +91 20 25902583; fax: +91 20 25893761.
E-mail addresses: shylesh19@gmail.com (S. Shylesh), ap.singh@ncl.res.in (A.P. Singh).

1381-1169/$ – see front matter © 2008 Elsevier B.V. All rights reserved.
doi:10.1016/j.molcata.2008.11.020

of different substrates [20–24]. The recent developments in heterogeneous MPV reduction reactions have been reviewed recently [25–27].

Periodic mesoporous organosilicas are remarkable organic–inorganic hybrid materials having organic moieties as molecularly bridging ligands in the frame wall positions; having a homogeneous distribution of organic fragments and silica moieties within the framework [28–30]. These materials show hydrophobic surfaces and consequently improve the hydrothermal stability applicable in diverse applications. Potential importance of organofunctionalized periodic mesostructures depends critically on the loading of accessible functional species in the network. Sulfonic acid functionalities for application in solid acid catalysis are reported whereas, amine functionalized hybrid mesoporous silicas finds their application in knoevenagel condensation reactions [31–35]. In addition, the titanium incorporated mesoporous hybrid silicas have demonstrated their potential in oxidative catalysis wherein the catalytic activity highly depends on the hydrophobicity of the materials [36–38]. Hence, in order to realize the full potential of the MPV reduction, the feasibility of supporting the aluminum isopropoxide over hydrophobic mesoporous organosilicas is attempted over the ethane (–CH_2–CH_2–) and ethene (–CH=CH–) bridged organosilicas and their stability was compared to a silylated mesoporous MCM-41 sample and conventional mesoporous silica supported $Al(O^iPr)_3$ catalyst (Scheme 1). Further, even though a variety of aluminum-containing catalyst was applied for MPV reduction, the truly active aluminum species is still not well understood and the stability of the supported aluminum isopropoxide is not high enough for practical applications. For instance, the aluminum isopropoxide catalyst exists as a tetra nuclear aggregate in the crystalline state in which the six-coordinated aluminum centre is surrounded by three bridging $Al(O^iPr)_3$ groups, but in solution a mixture of species forms and their easy interconversions complicates the prediction of active reactive aluminum sites [39]. Therefore, the heterogenization of aluminum isopropoxide over solid supports is alluring as they maintain the high activity with better reusability and thereby avoids the complications due to homogeneous catalysis. The work probes in detail about the influence of different supports in the grafting of aluminum isopropoxide species, effect of secondary alcohols used for the reduction, effect of poisoning agents in the catalytic activity and the nature of aluminum species formed over various support surfaces.

2. Experimental

2.1. Synthesis of aluminum doped PMS and PMO supports

Periodic mesoporous silicas (PMS) and organosilicas (PMO) were prepared by known literature procedures and were described in detail in The Supporting Information. The grafting of aluminum isopropoxide over mesoporous MCM-41 support was carried out as follows. Typically for 2 wt.% loaded MCM-41 support material (2Al@MCM-41), the support (1 g, previously activated at 200 °C/6 h) was added to 30 ml of dry hexane. A solution of aluminum isopropoxide (0.15 g) in dry hexane (50 ml) was then added to the support material slowly with vigorous stirring. The suspension was then stirred at 80 °C for 12 h. The concentration of aluminum isopropoxide in dry hexane was varied so as to obtain 5% and 10% aluminum in the mesoporous samples. The product obtained was then filtered, washed with hexane to remove any unreacted precursors. The material was then dried in vacuum and kept in a vacuum desiccator before it gets used in the reaction. A similar procedure was carried out over other supports like MCM-48, SBA-15, amorphous silica gel and organosilica samples and for the synthesis of vanadium-, titanium- and zirconium-grafted MCM-41 supports. The aluminum-grafted MCM-41 materials were denoted as *x*Al@MCM-41, where *x* stand for the input Al wt.%.

2.2. Characterization

PXRD patterns of the mesoporous samples were recorded on a Rigaku D MAX III VC instrument using Ni-filtered Cu Kα radiation, between 1.5° and 10° (2θ), with a scanning rate of 1°/min. The amount of carbon content was evaluated by elemental analysis using EA1108 Elemental Analyzer (Carlo Erba Instruments) and the amount of aluminum loading was determined by an inductively coupled-plasma optical-emission-spectrometer (ICP-OES), after solubilization of the samples in HF–HCl solutions. TEM analyses of the mesoporous samples were performed on a JEOL-JEM-1200 EX instrument, at an accelerated voltage of 120 kV. Nitrogen adsorption–desorption isotherms were measured at 77 K on a Quantachrome Autosorb 1 sorption analyzer after evacuation of the samples at 200 °C for 6 h. Pore size distribution (PSD) was obtained from the adsorption branch of the isotherm using Barrert–Joyner–Halenda (BJH) method. The nature of acid sites (Brönsted and Lewis) of metal-containing mesoporous catalyst was characterized by ex situ FT-IR spectroscopy with chemisorbed pyridine. A freshly activated catalyst powder sample was saturated with pyridine vapors placed in a desiccator containing pyridine. The pyridine-saturated sample was then activated at 150 °C for 2 h and the FT-IR spectra of the sample were recorded on a Shimadzu (Model-820PC) spectrometer under DRIFT mode. A similar procedure was used for the adsorption of cyclohexanone where instead of pyridine the probe molecule is changed to cyclohexanone. Solid-state ^{13}C CP MAS NMR, ^{29}Si MAS NMR and ^{27}Al MAS NMR spectra were recorded on a Bruker MSL 300 NMR spectrometer with a resonance frequency of 75.5, 59.6 and 104 MHz for ^{13}C, ^{29}Si and ^{27}Al using 4 mm zirconia rotors and a sample spinning frequency of 3 kHz. ^{13}C spectra were collected with 70° rf pulses, 5 s delay while ^{29}Si spectra were collected with 70° rf pulses, 30 s delay and in both cases with ~6000 scans. The chemical shifts were referenced to glycine, TMS and $[Al(H_2O)_6]^{3+}$ respectively, for ^{13}C and ^{29}Si and ^{27}Al.

2.3. Catalytic MPV reduction reactions

MPV reduction reactions were performed in a 10 ml round bottom flask immersed in a thermostated oil bath equipped with a

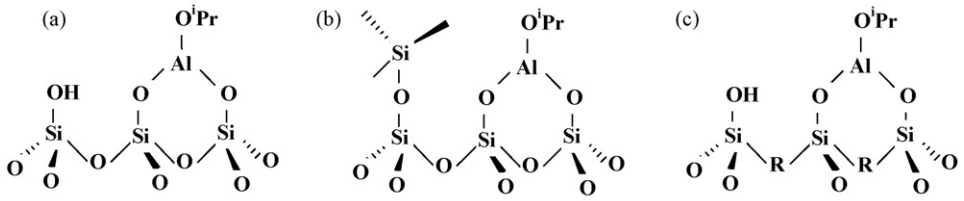

Scheme 1. Schematic representation of the grafting of $Al(O^iPr)_3$ catalyst over different mesoporous silica catalysts, (a) Si-MCM-41, (b) silylated Si-MCM-41 and (c) PMO.

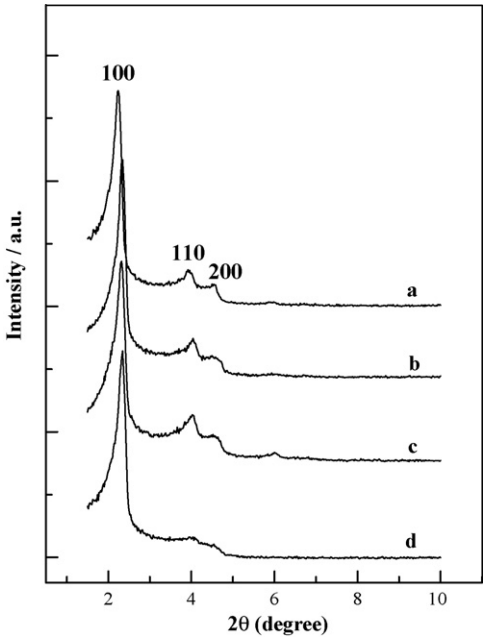

Fig. 1. XRD patterns of MCM-41 and aluminum isopropoxide-grafted samples; (a) Si-MCM-41, (b) 2Al@MCM-41, (c) 5Al@MCM-41 and (d) 10Al@MCM-41.

water-cooled condenser, septum port and a guard tube. 2-propanol and 2-butanol were freshly distilled and dried, before gets used in the reaction. In a typical reaction, 1 mmol of the substrate and 60 mmol of the alcohol were added to 100 mg of activated catalyst and the mixture was heated at temperatures between 85 and 100 °C, depending on the nature of secondary alcohol [24]. Aliquots were removed at different reaction times and the catalyst was separated from the reaction mixture by centrifugation. The products were analyzed on a gas chromatograph (HP 6890) equipped with a flame ionization detector (FID) and a capillary column (5 μm cross-linked methyl silicone gum, 0.2 mm × 50 m). The identity of the reaction products was verified by comparing the retention times and GC–MS (Shimadzu 2000 A) with authentic samples.

3. Results and discussion

3.1. Structural as well as textural features

XRD patterns of parent mesoporous MCM-41 silica and aluminum-grafted mesoporous MCM-41 samples of different aluminium loading are shown in Fig. 1. The pristine MCM-41 solid sample shows four Bragg reflexes with ($h\,k\,l$) reflections of (1 0 0), (1 1 0), (2 0 0) and (2 1 0) for a highly ordered hexagonal symmetry. After grafting aluminum isopropoxide, the width of the (1 0 0) peak gets narrowed which may relate to the more homogenous distribution of the pore structure brought about by the attachment of $Al(O^iPr)_3$ groups inside the mesopore channels. In addition, with an increase in the percentage of aluminum grafting, a slight decrease in the peak intensity and a gradual decrease in the d_{100} value is noted, showing the reduction in the pore size with the percentage of aluminum loading. The decrease in intensity of the d_{100} peak and long range ordered peaks is a common phenomenon observed in mesoporous materials, during post synthesis modifications, and are attributed to the partial structural collapse of the mesoporous structure or to the flexibility induced in the silica framework due to the strain generated from the grafted species [40,41]. Similar to MCM-41, Si-SBA-15 and aluminum-grafted 10Al@SBA-15 samples also shows three ($h\,k\,l$) reflections of (1 0 0), (1 1 0) and (2 0 0) in the 2θ range of 0.8°–2° indexed to two-dimensional (2D) hexagonal *p6mm* symmetry, indicating a highly ordered hexagonal structure. However, Si-MCM-48 and its aluminum analogue show two main peaks relating to the (2 1 1) and (2 2 0) reflexes of the cubic structure (Fig. S1, Supporting Information) [23]. The presence of characteristic reflections even after 10% aluminum loading for all the PMS samples suggest that the mesoporous materials are ordered with uniform pore arrangements and the grafting process had not damaged the pore structure of the mesoporous materials. Similarly, the PMO samples also show the characteristic peaks relating to the hexagonal structure and after aluminum grafting a decrease in intensity of the d_{100} peak is observed. The d spacing values of all aluminum-containing samples are listed in Table 1. Further evidence for the retainment of ordered structural features over the mesoporous materials after $Al(O^iPr)_3$ grafting reactions are directly provided from the TEM images (Fig. S2, Supporting Information). TEM of pristine mesoporous SBA-15, MCM-41 and organosilica samples shows the images of channels and framework when the electron beam is passed perpendicular to the pore, demonstrating a highly ordered pore structure, akin to the ordered structure as observed from XRD patterns. After aluminum grafting, a slight disordering in the pore channels of mesoporous materials was observed, showing the retainment of pore architecture after the grafting of $Al(O^iPr)_3$ species.

The amount of aluminum-grafted over different support samples was determined by the ICP-OES analysis. The percentage loading of aluminum was found to be almost similar over all the periodic mesoporous silica materials. Among them, Si-MCM-41 shows the highest amount of aluminum grafting revealing a greater percentage of silanol groups for the stabilization of aluminum species. Contrary, the PMO sample shows a decreased amount of aluminum grafting than the mesoporous silica samples. This result shows that the number of silanol groups available for grafting is different for the silicas and organosilicas and thus the unstabilized aluminum species in organosilica samples get washed out during the filtration steps. Thus the low percentage of aluminum observed for the ethane–silica and ethene–silica samples relate to the limited accessibility of the surface hydroxyl groups for the $Al(O^iPr)_3$ species or due to the different surface properties between the two classes of mesoporous solid materials (Table 1). In addition, elemental analysis results obtained from the percentage of carbon (CHN analysis)

Table 1
Chemical and textural properties of mesoporous silica supported aluminum catalysts.

Sample	Al (%)[a]	d spacing (nm)[b]	S_{BET} ($m^2\,g^{-1}$)	Pore volume ($cc\,g^{-1}$)	Pore diameter (nm)
10Al@MCM-41	6.2	3.5	636	0.52	2.3
10Al@MCM-48	5.8	3.3	758	0.59	2.5
10Al@SBA-15	5.3	10.5	689	0.82	6.7
10Al@SG	4.8	–	377	0.46	4.2
10Al@EE-SI	4.7	3.5	385	0.30	2.5
10Al@ET-SI	4.4	3.3	325	0.31	2.4

SG = silica gel, EE-SI = ethane–silica, ET-SI = ethene–silica.

[a] Determined by ICP analysis.

[b] Unit cell parameter can be calculated from, $a_0 = 2d_{100}/\sqrt{3}$ (MCM-41, SBA-15, EE-SI, ET-SI) and $a_0 = d_{211}/\sqrt{6}$ (MCM-48).

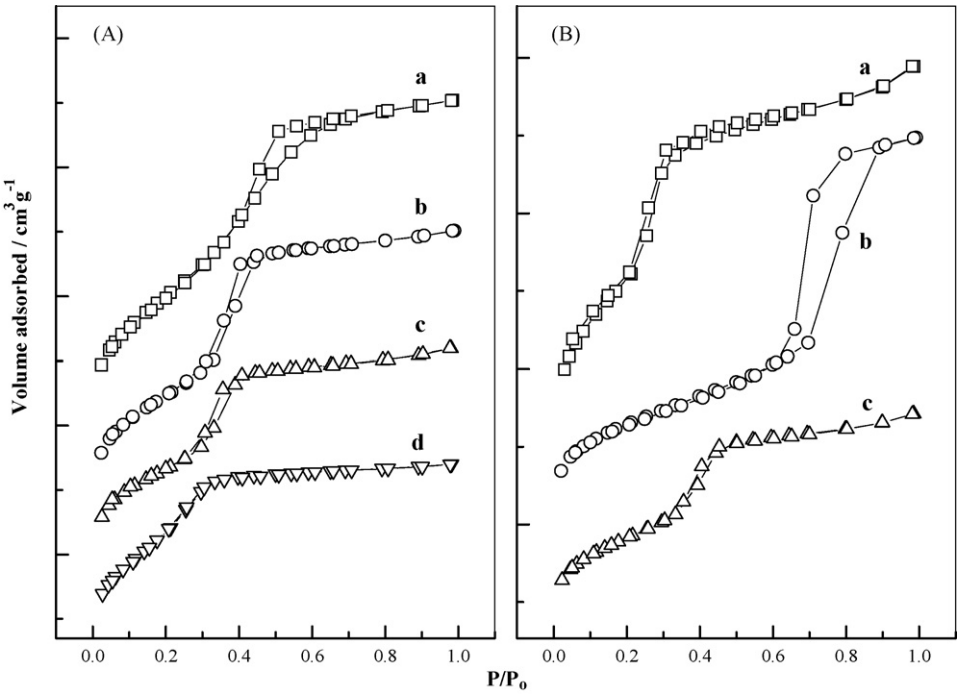

Fig. 2. Nitrogen adsorption–desorption isotherms of (A) (a) Si-MCM-41, (b) 2Al@MCM-41, (c) 5Al@MCM-41, (d) 10Al@MCM-41 and (B) (a) 10Al@MCM-48, (b) 10Al@SBA-15, (c) 10Al@EE-SI.

and aluminum (ICP), shows a ligand/metal ratio of ~2. This result suggests that two isopropoxide groups of Al(O^{i}Pr)$_3$ get anchored to the mesoporous silica surface (silanol groups) with the removal of propanol groups.

The textural characteristics of aluminum-grafted mesoporous samples were evaluated from the low temperature nitrogen adsorption–desorption isotherms (Fig. 2). N_2 isotherm of aluminum-containing MCM-41, MCM-48 and organosilica samples display type IV isotherms with a sharp capillary condensation step at P/P_o = 0.3–0.4, characteristics of mesoporous materials having uniform mesopore structure. Compared to the pristine MCM-41 silica support, the capillary condensation steps of aluminum-grafted mesoporous samples of different loadings gets reduced to lower P/P_o values, suggesting a reduction in the pore size, and are in agreement with the shifting of XRD d_{100} peak to higher 2θ values after aluminum grafting [41]. The capillary condensation step is prominent for all the grafted samples, which suggest a narrow, pore size distribution for the mesoporous samples. The aluminum-grafted, 10Al@SBA-15 sample show a sharp increase in the N_2 adsorption step at a higher P/P_o value (~0.7) with a distinct hysteresis loop of an almost parallel adsorption and desorption (Type H1) step [42]. The textural properties, such as the specific surface area, pore volume and pore sizes are further given in Table 1. The support Si-MCM-41 sample shows a high surface area of 886 m^2 g^{-1}, pore volume of 0.77 cc g^{-1} and pore diameter of 3.1 nm while the 10% aluminum-grafted 10Al@MCM-41 sample shows a surface area of 819 m^2 g^{-1}, pore volume of 0.68 cc g^{-1} and a pore diameter of 2.9 nm. The reduced pore diameter together with the retention of structural ordering suggests that aluminum isopropoxide species are uniformly grafted over the support samples. A comparison in the pore size reduction after 10% Al grafting shows that the reduction is lower over the SBA-15 sample followed by Si-MCM-48, Si-MCM-41 and organosilica samples (Table 1). The small shrinkage in pore size of SBA-15 sample possibly relates to the thicker pore walls of the SBA-15 support than the thin pore walls of the M41S or organosilica samples [42]. Noteworthy, the mesoporous organosilica samples show a large decrease in the textural properties after aluminum loading and are in particular for the ethene–silica sample. This may arise due to the low structural stability of the ethene–silica than the ethane–silica sample and hence higher amounts of Al(O^{i}Pr)$_3$ groups may disturbed the mesopore structure, as noted from the XRD patterns [43].

3.2. NMR investigation of mesoporous samples

^{13}C CP MAS NMR of surfactant-extracted ethane–silica sample shows the presence of a single, sharp peak at 5.4 ppm for the ethane (–CH$_2$–CH$_2$–) functional groups integrated in the wall channels of the hybrid materials. Meanwhile, the ethene–silica sample shows a sharp peak at 145 ppm assigned to the ethylene (–CH=CH–) functional groups linked to the silicon [28–30]. Moreover, carbon NMR confirmed the absence of peaks in the range 10–60 ppm of the surfactant species (Fig. S3, Supporting Information). This result indicates that the surfactant groups are removed from the pores of the hybrid sample by employing the two time extraction procedures. ^{29}Si MAS NMR of calcined mesoporous PMS samples show the presence of broad resonance peaks from −90 to −110 ppm, indicative for a range of Si–O–Si bond angles and the formation of more tetrahedral silicon environments. The peaks observed at −110, −101, −92 (sh), are usually assigned to the Q^4 (Si(OSi)$_4$), Q^3 (Si(OH)(OSi)$_3$), and Q^2 (Si(OH)$_2$(OSi)$_2$) sites, respectively. Compared to parent silica samples, Al(O^{i}Pr)$_3$-grafted mesoporous silica materials shows a decrease in the Q^3 and Q^2 values with a corresponding increase in the percentage of Q^4 sites, showing that Al(O^{i}Pr)$_3$ effectively consumes the geminal as well as the free silanol sites (Fig. S4, Supporting Information). In general, the Q^3 sites are considered to be rich with isolated Si–OH groups, which may be free or hydrogen bonded, while the Q^2 sites posses the geminal silanol sites. A decrease in the Q^3 and Q^2 values after grafting reactions, over all the support materials, shows that these silanol groups are highly accessible to the Al(O^{i}Pr)$_3$ groups [40]. Among the support samples, the higher $Q^3 + Q^2/Q^4$ ratio in MCM-41 (0.59) indicates that they possesses abundant silanol groups than SBA-15 (0.47) and silica gel (0.33) and these results explains the higher

$Al(O^iPr)_3$ loading over MCM-41 sample than the other two samples. ^{29}Si MAS NMR spectra of organosilica samples (ethane–silica and ethene–silica) show the presence of two peaks; one at −57 ppm for the T^2 sites ($C(OH)Si–(OSi)_2$) and the other at −68 ppm for the T^3 sites ($CSi–(OSi)_3$). Absence of Q^n sites (−90 to −110 ppm) clearly shows that no Si–C bond cleavage had occurred during the extraction process (Fig. S3, Supporting Information) [28–30]. Besides, the relative intensity of the peaks suggest that the organosilica samples possess a significant proportion of T^3 silicon environments, which in turn accounts for their better stability and also shows that sufficient silanol groups are available for post synthesis modifications. Akin to mesoporous silica, the organosilica samples also shows a decrease in the percentage of T^2 sites after aluminum grafting with a corresponding increase in the T^3 sites. All these results suggest that $Al(O^iPr)_3$ groups gets grafted over the mesoporous supports utilizing the Q^3 and Q^2 silanol sites of mesoporous silica samples and T^2 sites of the mesoporous organosilica samples. However, the decreased percentage of aluminum grafting over the organosilica sample possibly relates to the inherent surface property difference between the periodic mesoporous silicas and organosilicas.

It is known that apart from appropriate Lewis acidity, the catalytic efficiency in MPV reduction reaction depends on the coordination geometry of the active aluminum sites [44]. As mentioned in Section 1, aluminum isopropoxide is known to exist either as trimer or as tetramer. The structure of the tetrameric form is anticipated to be associated with a central octahedrally coordinated aluminum atom bonded by twin oxygen bridges to three tetrahedrally coordinated aluminum atoms [39]. Hence, in order to determine the coordination state of aluminum and to know–how the aluminum species gets stabilized over the different silica support surfaces, ^{27}Al MAS NMR measurements were performed and were compared with the pure $Al(O^iPr)_3$ (Fig. 3). The results provide useful insights into coordination geometry of the catalytically active species. Solid-state NMR spectra of $Al(O^iPr)_3$ show an intense peak at 0 ppm, typical of the octahedral aluminum, along with a small peak at chemical shift of 58 ppm attributable to the tetrahedral aluminum. Whereas, the PMOs and MCM-41-grafted aluminum species displays two sharp peak maxima at 45–55 ppm, for the distorted tetra- or penta-coordinated aluminum sites, and at 0 ppm, for the octahedral sites (Fig. 3). However, no difference in the peak positions is observed for the different percentage aluminum-grafted samples, *viz*., 2Al@MCM-41, 5Al@MCM-41 and 10Al@MCM-41, but the peak intensities gets increased with aluminum grafting. The organosilica-grafted aluminum samples also show an identical pattern as that of 10Al@MCM-41. Further, compared to the M41S and organosilica-grafted $Al(O^iPr)_3$ samples, the silica gel-grafted aluminum samples show a higher intense octahedral peak and the peak relating to the tetra- or penta-coordinated species is very less. Aforementioned different aluminum sites formed over mesoporous supports upon grafting of $Al(O^iPr)_3$ fairly supports a disruption of the tetrameric form during grafting. In an earlier report, it was mentioned that the melt form of $Al(O^iPr)_3$ consists predominantly trimeric species with tetra- or penta-coordinated aluminum species and are found more reactive in the MPV reductions than the tetrameric form containing tetra- or hexa-coordinated aluminum. Besides, Shrinker and Wittaker pointed out that alcohols like isopropanol, accelerates the depolymerization of the tetramer to the melt form and hence we probed the ^{27}Al MAS NMR of the spent 10Al@MCM-41 catalysts [45]. However, a retainment in the peak intensity and peak position is noted showing that the possible state of $Al(O^iPr)_3$ be the trimeric form than the tetrameric form and hence we anticipate that the lower coordinated trimeric species anchored over the mesoporous silica support may results in the better catalytic activity of the aluminum-grafted mesoporous samples. Therefore, an improved catalytic activity of the $Al(O^iPr)_3$-grafted mesoporous materials is highly anticipated in the MPV reduction. It could be also proposed that geometrically distorted 4- or 5-coordinated aluminum species, and the pore confinement effects of mesoporous hosts would accelerates the catalytic activity in the MPV reduction (next section).

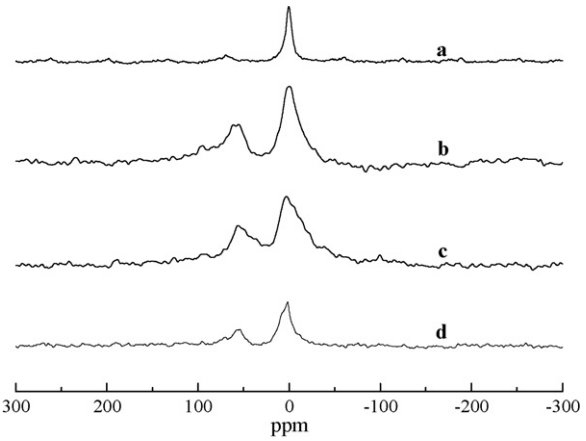

Fig. 3. ^{27}Al MAS NMR results of, (a) $Al(O^iPr)_3$, (b) 10Al@ MCM-41, (c) 10Al@EE-SI, and (d) 10Al@SG.

3.3. Catalytic MPV reduction reactions

Transition metal catalyzed heterogeneous hydrogen transfer reactions from secondary alcohols to carbonyl compounds are interesting since these procedures avoids the use of high pressure molecular hydrogen or hazardous reduction reagents like $LiAiH_4$ and $NaBH_4$ [18]. Moreover, the heterogeneous solid supported catalyst offers further advantages like the easy catalyst and product recovery as well as a possible reuse of the catalyst systems. Hence mesoporous materials were selected for the hydrothermal synthesis and grafting of aluminum species due to their potential for incorporating higher amounts of heteroatoms in the frame wall positions as well as due to the presence of higher amounts of silanol groups, for the stabilization of aluminum isopropoxide. The hydro thermally synthesized aluminum-containing Al-MCM-41 and Al-PMO samples were first applied as catalysts for the MPV reduction reaction of cyclohexanone. Results showed that even after 24 h, both the catalysts show less conversion (<5%) and would indicate that the Lewis acidity is not strong enough and/or the amount of framework aluminum is small to proceed the reaction effectively. Hence, $Al(O^iPr)_3$-grafted mesoporous MCM-41 samples with different percentage of aluminum loading *viz*. 2%Al, 5%Al and 10%Al were synthesized and were applied in the MPV reduction of cyclohexanone using 2-propanol as well as 2-butanol as the hydrogen transfer agents. The rate of reaction was found to get increased with the percentage of aluminum loading and the catalyst containing 10%Al shows the highest conversion. An interesting result was that the selectivity towards the reduced product was >98% in the presence of all catalysts even after 24 h, showing that the supported aluminum catalysts are highly selective. The resulted improved conversion for 10Al@MCM-41 catalyst shows that $Al(O^iPr)_3$ is grafted as a monolayer over the support surface and the higher concentration of aluminum helps to increase the number of Lewis acid sites for the conversion of cyclohexanone. Comparing these results with the Al-beta zeolites it was inferred that the zeolite catalysts enhance undesired side reactions due to the presence of Lewis and Brönsted acidity, generated after the calcination process [18]. However, the absence of undesired side products even after 24 h, for the 10% Al-grafted mesoporous materials suggest that polarization of carbonyl groups gets enhanced over the Lewis acid sites or Lewis acid sites be the active catalytic

Table 2
MPV reduction of cyclohexanone over aluminum-containing mesoporous silica catalysts.

Catalyst	Conversion of cyclohexanone (mol.%)	
	2-propanol	2-butanol
10Al@MCM-41	87	96
10Al@MCM-48	76	97
10Al@SBA-15	58	64
10Al@SG	39	51
10Al@EE-SI	58	62
10Al@ET-SI	50	53
$Al(O^iPr)_3$	70	85

Reaction conditions: substrate, 1 mmol; 2-butanol/2-propanol, 50 mmol; *T*, 100 °C (2-butanol) and 85 °C (2-propanol); *t*, 12 h; catalyst wt., 100 mg. Selectivity for cyclohexanol in all cases is 100%.

Table 3
Selective reduction of cyclohexanone over different hydrogen transfer agents and different metal-grafted MCM-41 samples.

Catalyst	Conversion (mol.%)			
	2P	2B	CP	MC
10Al@MCM-41	87	96	73	62
10Zr@MCM-41	81	95	78	65
10Ti@MCM-41	24	36	n.d	n.d
10V@MCM-41	nil	2	nil	nil

Reaction conditions: substrate, 1 mmol; 2-butanol/2-propanol, 50 mmol; *T*, 100 °C (2-butanol) and 85 °C (2-propanol); *t*, 12 h; catalyst wt., 100 mg. 2B = 2-butanol, 2P = 2-propanol, CP = cyclopentanol and MC = methyl cyclohexanol. Selectivity for cyclohexanol in all cases is 100%. n.d = not determined.

sites. Moreover, as pointed out by Anwander et al., the surface confinements effects in mesoporous hosts may prevents the aluminum alkoxide groups from self-association while the silicate material simultaneously acts as an electron-withdrawing matrix [44]. The decreased activity of the silica gel supported aluminum catalyst also holds this explanation (Table 2).

A series of secondary alcohols was tested for the MPV reduction of cyclohexanone using 10Al@MCM-41 as catalyst (Table 3). It can be seen from table that among the secondary alcohols tried, 2-butanol shows higher cyclohexanol yield followed by 2-propanol, cyclopentanol and methyl cyclohexanol. For instance, in the presence of 2-butanol, the 10Al@MCM-41 catalyst showed a conversion of 96% while under 2-propanol, cyclopentanol and methyl cyclohexanol the conversions are 87%, 73% and 62%, respectively, after 12 h run. Corma et al. observed a similar effect over Sn-beta zeolites and had attributed that the lower activity is not related to the pore diameter limitations of the zeolites but the shielding effect of the oxygen bonded to the Sn atoms, when increasing the diameter of the secondary alcohols [21]. In addition, the formation of transition state with the bulky secondary alcohols may be less and thus the coordination of such large molecules to the Lewis sites is more limited than *sec*-alcohols like 2-butanol. These interpretations are consistent with the lower activity observed over the homogeneous $Al(O^iPr)_3$ catalyst when cyclopentanol was used in the reduction process and shows that the geometrical limitations for the formation of transition state over Lewis acid sites, significantly alters the yield of ketone products.

Substituted cyclohexanones like 2-, 3-, 4-methyl cyclohexanone and 4-*tert*-butyl cyclohexanone were also reduced, to the corresponding *trans*- and *cis*-alcohols, using 10Al@MCM-41 catalysts, in the presence of 2-propanol and 2-butanol (Table 4). Like cyclohexanone, the conversion as well as the selectivity to the *trans* product was found more under 2-butanol hydrogen source. Moreover, among the substituted cyclohexanones, the 4-substituted substrates show maximum conversion results that 4-*tert*-butyl cyclohexanone also reduces to the same extent to that of cyclohexanone even though bulky groups are present in the chain. Creyghton et al. observed the significant formation (>90%) of thermodynamically less favored *cis*-isomer in the presence of zeolite catalysts [11]. However, aluminum-grafted mesoporous catalysts show the predominant formation of *trans* product with selectivity greater than 95%, except 2-methyl cyclohexanone. No other reaction (condensed) products are observed, showing that the aluminum-grafted mesoporous catalysts are highly selective. The higher stereo selectivity observed with the zeolite catalysts (Sn-beta, Zr-beta and Ti-beta) shows that the reaction proceeds in the zeolite pore channels and the steric constraints force the reaction to proceed *via* the less bulky transition state [18]. However, the larger pore channels of the mesoporous silica hosts as well as the amorphous pore channels enhance the formation of the *trans*-isomer than the *cis*-isomer product.

3.3.1. Influence of different supports

In order to observe whether the structural and textural features of the support material, had any effect in the conversion of cyclohexanone, aluminum isopropoxide (Al 10%) was grafted over a series of periodic mesoporous silica samples (MCM-41, MCM-48 and SBA-15) and periodic mesoporous organosilica samples like the ethane–silica and ethene–silica and an amorphous silica gel sample (Table 2). Among the support samples, 10Al@MCM-41 shows the maximum conversion followed by 10Al@MCM-48 and 10Al@SBA-15, in the presence of 2-propanol. Interestingly, the same amount loaded over a silica gel sample shows lower conversion of 29% after 12 h reaction and the hybrid organosilica samples also show lower conversion of 58% and 50% for ethane–silica and ethene–silica, respectively, after 12 h. These results show that the structural features of the support material affects the catalytic activity of the aluminum catalysts that the one-dimensional channel oriented support shows slightly higher activity than the three-dimensionally channel oriented MCM-48 sample and the large pore SBA-15 sample. The reason for the lower activity observed for SBA-15 sample may be due to the presence of micropores in the samples where the aluminum isopropoxide-grafted may block these pores and

Table 4
Comparative MPV reduction of substituted cyclohexanone over 10Al@MCM-41.

Catalyst	Substrate	Conversion (mol.%)	Selectivity (mol.%)	
			–ol (*trans*:*cis*)	Others
10Al@MCM-41 (2-propanol)	2-methyl cyclohexanone	38	72/28	0
	3-methyl cyclohexanone	17	8/92	0
	4-methyl cyclohexanone	50	95/5	0
	4-tert-butyl-cyclohexanone	55	92/8	0
10Al@MCM-41 (2-butanol)	2-methyl cyclohexanone	70	63/37	0
	3-methyl cyclohexanone	73	>99 (*cis*)	0
	4-methyl cyclohexanone	82	>99	0
	4-tert-butyl-cyclohexanone	92	87/13	0

Reaction conditions: substrate, 1 mmol; 2-butanol/2-propanol, 50 mmol; *T*, 100 °C (2-butanol) and 85 °C (2-propanol); *t*, 12 h; catalyst wt., 100 mg.

had limited access for the substrate molecules for the formation of transition state species. Similarly, in the presence of 2-butanol also the conversion followed a similar trend that the M41S related samples show a higher conversion than the SBA-15, silica gel and the aluminum-grafted mesoporous organosilica samples. However, normalization of the MPV reduction activities with actual aluminum incorporation determined by ICP analysis (Table 1), revealed no significant differences in MPV catalytic activities between PMOs and conventional M41S type mesoporous materials.

3.3.2. Influence of different metal alkoxides

For comparison, vanadium isopropoxide, titanium isopropoxide and zirconium propoxide (all ~10%) was loaded over MCM-41 and was also used as catalysts in the presence of both 2-propanol and 2-butanol (Table 3). Vanadium-grafted mesoporous catalysts show no conversion even after 12 h reaction while the titanium- and zirconium-grafted mesoporous catalysts show a conversion of 24% and 81%, respectively, after 12 h run, in the presence of 2-propanol and shows a conversion of 36% and 95%, respectively, in the presence of 2-butanol. These results are in well accordance with the observation of Zhu et al. that supported zirconium propoxide are efficient catalyst for the MPV reduction reactions [24]. The better catalytic activity of the aluminum isopropoxide-grafted catalyst than the titanium and vanadium-grafted catalysts can be explained from the FT-IR pyridine adsorption studies. The amount and strength of Lewis acid sites of the metal (Al, Zr, Ti and V) containing MCM-41 samples were compared by means of IR spectroscopy (1200–1800 cm^{-1}) after adsorption of pyridine at room temperature and desorption at 150 °C (Fig. S5, Supporting Information). The band at 1450 cm^{-1} indicates the presence of Lewis acid sites for the samples containing Al, Zr and Ti. A comparison of the spectra shows that the aluminum-grafted sample posses large amounts of Lewis and Brönsted acidity, while zirconium and titanium show an almost similar spectrum. However, the intensity of the peaks is higher over zirconium containing sample than the titanium sample. Interestingly, mesoporous MCM-41 containing vanadium shows negligible or no adsorption of pyridine associated to Lewis acid sites after desorption at 150 °C. All the above result suggests that the interaction of carbonyl groups with the Al and Zr-containing MCM-41 samples is stronger than the Ti and V-containing samples. Thus even though residual Brönsted acid sites are also present in aluminum-grafted mesoporous samples, the absence of undesired reactions suggest that Lewis acid sites of definite strength are actually promoting the reaction and the presence of residual Brönsted sites had little effect in the selectivity of desired products in MPV reactions. We also performed the IR spectra of the 10Al@MCM-41 catalyst which adsorbed cyclohexanone at room temperature and desorbed at 150 °C (figure not shown). At room temperature, the sample shows a sharp signal at 1720 cm^{-1}, relating to the carbonyl vibration of the ketone group and a small signal at 1675 cm^{-1}. However, after desorption at 150 °C, a shift of this band to lower wave number (~30 cm^{-1}) was noted, indicating the formation of an adduct with the carbonyl groups of the cyclohexanone and the aluminum sites. The intensity of the signal was found to get decreased with an increase in the temperature and at 200 °C, the signal at 1720 cm^{-1} disappeared almost completely with retention of the band observed at 1675 cm^{-1}, showing the strong dative bond from the carbonyl oxygen to the Al-sites of the grafted samples. However, the titanium- and vanadium-grafted samples show only a slight shift of 20% and 8%, respectively, to lower wave numbers. These results are similar to the results observed for the Sn-beta, Ti-beta and Si-beta zeolites [20,21]. Thus a combination of both the IR result suggests that for the MPV reaction to initiate an appropriate Lewis acidity is needed so that the carbonyl groups can coordinate and help in its right polarization. Thus the poor catalytic activity of vanadium-grafted mesoporous catalysts in the MPV reactions is attributed to the poor Lewis acid character of these materials or that the Lewis acidity is not sufficient for the polarization of the carbonyl groups so as to initiate the reactions [20]. Hence, appropriate Lewis acidity, as judged from the IR measurements and pore confinement effect possibly correlates the high activity and selectivity of the aluminum-grafted mesoporous samples.

3.3.3. Poisoning experiments

One of the major drawbacks of M41S related mesoporous support is its decreased hydrothermal stability. Hence in the present study, hydrophobic supports like the ethane–silica and ethene–silica mesoporous organosilica supports were synthesized for the grafting reactions. These supports had shown higher hydrothermal stability than the M41S related materials, due to the improved hydrophobicity imparted from the presence of integrated organic groups in the frame wall positions (Fig. S6, Supporting Information) [46]. Hence, as a first experiment, the effect of water in the catalytic activity of the hybrid materials was evaluated. The catalyst 10Al@MCM-41 kept under ambient conditions was applied in the reduction reaction of cyclohexanone, which shows a conversion of 75% after 12 h. However, when the activation temperature was increased to 150 °C, the conversion of the 10Al@MCM-41 sample gets increased to 90% after 12 h. TG-DTG analysis of the former sample (hydrated) shows that water gets removed below 120 °C and hence the decreased activity of the sample in the earlier case can be reasonably attributed to the poisoning effect of the atmospheric water on the active aluminum sites. However, the continuance of an almost similar conversion after activating the catalysts at 150 °C shows that the aluminum isopropoxide groups are not hydrolyzed and the physisorbed atmospheric water molecules get expelled off and thus become available for the reactant species to gets coordinated. In order to confirm the role of water in the deactivation of catalysts, as a second experiment, different percentage of water was deliberately added to the reaction mixture after activation of the catalyst at 150 °C for 12 h. Results show that addition of 0.1 g of water to the reaction mixture decreased the conversion of 10Al@MCM-41 catalyst from 96% to 48% and after the addition of 0.5 g water, a complete loss in the catalytic activity was observed (Table 5). The sudden conversion drop in the presence of high amount of added water may relate to the blocking of active aluminum sites or due to the hydrolysis of the aluminum isopropoxide groups under high temperature reaction conditions. These results highlight the poisoning effect of water in the MPV reactions and thus show that for practical applications of aluminum supported mesoporous silica catalysts, the samples should be carefully activated before applying to the reaction medium, apart from the drying of the reagents.

Noting this deactivation for the 10Al@MCM-41 catalysts in the presence of added water, we silylated the 10Al@MCM-41 catalyst using $(CH_3)_2Si(OC_2H_5)_2$, in the viewpoint that the presence of organic groups enhance the stability of the grafted aluminum species [47]. Even though the conversion gets decreased, the water tolerance was found better (85% decreased to 15%, after 12 h run) than the non-silylated aluminum catalyst, even when 10 wt.% of water was present in the reaction medium (Table 5). Thus the enhancement in the stability of the silylated 10Al@MCM-41 catalyst having hydrophobic environments, prompted us to use aluminum-grafted hydrophobic ethane–silica and ethene–silica as catalyst for the MPV reaction. Recent reports also show that the organosilica samples had higher hydrophobic feature than the conventional mesoporous silica due to the presence of integrated organic groups in the frame wall positions [31–38]. Accordingly, the aluminum-containing mesoporous organosilica catalyst retains a higher activity and improved water resistance than the conventional mesoporous silica materials, showing the stable anchoring of the $Al(O^iPr)_3$ moieties over the hydrophobic mesoporous organosilica supports compared to M41S materials (Table 5). In addition, in

Table 5
Effect of different poisoning agents in the MPV reaction over aluminum-grafted mesoporous samples.

Catalyst	Poisoning agent	Conversion (mol.%)	Selectivity (mol.%)
10Al@MCM-41	Water (2 wt.%)	38	100
	Water (4 wt.%)	15	100
	Water (10 wt.%)	<1	100
	Pyridine	42	100
Sil-10Al@MCM-41[a]	Water (2 wt.%)	51	100
	Water (10 wt.%)	12	100
10Al@EE-SI	Water (2 wt.%)	47	100
	Water (10 wt.%)	34	100

Reaction conditions: substrate, 1 mmol; 2-butanol, 50 mmol; *T*, 100 °C; *t*, 12 h; catalyst wt., 100 mg.
[a] Silylated sample using $(CH_3)_2Si(OC_2H_5)_2$.

order to verify the role of active Lewis sites, selective poisoning experiments were carried out over the 10Al@MCM-41 catalysts. For that purpose, small amount of pyridine was added to the reaction mixture and are applied to the reaction conditions as stated in the experimental section. The addition of pyridine decreases the rate of the reaction drastically showing that pyridine is adsorbing to the Lewis sites, and thereby retards further coordination of the substrate to the active Al-sites for the formation of transition state. These results, together with the FT-IR results confirm that Lewis acidic aluminum centers are the active catalytic sites for the MPV reaction over the $Al(O^iPr)_3$ supported mesoporous catalysts. Hence, a further tuning in the synthesis procedures by which if the amount of aluminum can be increased over the PMO supports; a water tolerant, highly active aluminum supported mesoporous catalyst can be prepared.

3.3.4. Recycling studies

The heterogenity of the $Al(O^iPr)_3$ supported mesoporous silica and organosilica catalyst was determined by two different ways. As a first method, the catalyst was reused under similar experimental conditions, but after washing the catalyst with copious amounts of 2-butanol and drying at 150 °C for 12 h. The grafted catalyst can be reused up to four times with similar activity and selectivity. Further, the filtrate obtained after refluxing the grafted catalyst in 2-butanol was not active for the MPV reduction reactions, showing the absence of leached aluminum into the reaction medium. Both these results confirm that the aluminum isopropoxide-grafted mesoporous organosilicas are active, selective and stable catalyst for the MPV reduction reactions and are not prone to significant leaching under the current experimental conditions.

4. Conclusions

In summary, aluminum isopropoxide-grafted mesoporous organosilicas is an efficient and ultra stable catalyst for the MPV reduction of carbonyl groups in the presence of 2-butanol as hydrogen transfer agent than the conventional mesoporous silica doped aluminum catalysts. Among the different metal alkoxide used, aluminum and zirconium alkoxide supported mesoporous hosts show an almost similar conversion followed by titanium- and vanadium-grafted mesoporous silica. The low activity of vanadium-grafted sample is attributed to the poor Lewis acidity of the vanadium sites for the polarization of the carbonyl groups. Reactions over a series of various substrates show that the ease of formation of the transition state intermediate as well as the structural properties of the reducing agents influences the yield of the reduced products. The results revealed that appropriate Lewis acidity along with facile ligand exchange property are necessary for improved catalytic activity. Preferably 4- or 5-coordinated state of aluminum is appropriate to create required Lewis acidity to facilitate the MPV reduction. Additional insights into the catalytic stability of the materials can be rely on the choice of improved reaction parameters such as the careful drying of the solvents, proper activation of the catalyst as well as preparing more hydrophobic mesoporous supports for the grafting reactions.

Acknowledgements

The authors are grateful to Mr. R.K. Jha, for adsorption measurements, Mrs. Renu Parischa, for the TEM analysis, and Mrs. Kavitha, for the NMR analysis. S.S. thanks CSIR, India, for a senior research fellowship and acknowledges the task force project ("Catalysts and Catalysis"/P23-CMM 0005-B) by CSIR India for financial assistance.

Appendix A. Supplementary data

Supplementary data associated with this article can be found, in the online version, at doi:10.1016/j.molcata.2008.11.020.

References

[1] C.F. deGraauw, J.A. Peters, H. van Bekkum, J. Huskens, Synthesis 10 (1994) 1007.
[2] D. Klomp, T. Maschmeyer, U. Hanefeld, J.A. Peters, Chem. Eur. J. 10 (2004) 2088.
[3] R. Cohen, C.R. Graves, S.-B.T. Nguyen, J.M.L. Martin, M.A. Ratner, J. Am. Chem. Soc. 126 (2004) 14796.
[4] T. Ooi, T. Miura, Y. Itagaki, H. Ichikawa, K. Maruoka, Synthesis 18 (2002) 279.
[5] K.G. Akamanchi, N.R. Varalakshmy, Tetrahedron Lett. 36 (1995) 3571.
[6] M.A. Aramendia, V. Borau, C. Jimenez, J.M. Marinas, J.R. Ruiz, F.J. Urbano, J. Colloid Interf. Sci. 238 (2001) 385.
[7] E.J. Campbell, H. Zhou, S.T. Nguyen, Org. Lett. 3 (2001) 2391.
[8] T. Ooi, T. Miura, K. Maruoka, Angew. Chem. Int. Ed. 37 (1998) 2347.
[9] A. Lebrun, J.L. Namy, H.B. Kagan, Tetrahedron Lett. 32 (1991) 2355.
[10] J.L. Namy, J. Souppe, J. Collin, H.B. Kagan, J. Org. Chem. 49 (1984) 2045.
[11] E.J. Creyghton, S.D. Ganeshie, R.S. Downing, H. van Bekkum, J. Mol. Catal. A Chem. 115 (1997) 457.
[12] J.C. van der Waal, P.J. Kunkeler, K. Tan, H. van Bekkum, J. Catal. 173 (1998) 74.
[13] J.C. van der Waal, E.J. Creyghton, P.J. Kunkeler, H. van Bekkum, Top. Catal. 4 (1997) 261.
[14] J.C. van der Waal, M.S. Rigutto, H. van Bekkum, Chem. Commun. (1994) 1241.
[15] P.J. Kunkeler, B.J. Zurdeeg, J.C. vander Waal, J.A. van Bokhoven, D.C. Koningsberger, H. van Bekkum, J. Catal. 180 (1998) 234.
[16] M.A. Aramendia, V. Borau, C. Jimenez, J.M. Marinas, F.J. Romero, Catal. Lett. 58 (1999) 53.
[17] M.A. Aramendia, V. Borau, C. Jimenez, J.M. Marinas, J.R. Ruiz, F.J. Urbano, Appl. Catal. A Gen. 244 (2003) 207.
[18] J. Lopez, J.S. Valente, J.M. Clacens, F. Figueras, J. Catal. 208 (2002) 30.
[19] J.R. Ruiz, C.J. Sanchidrian, J.M. Hidalgo, J.M. Marinas, J. Mol. Catal. A Chem. 246 (2005) 190.
[20] A. Corma, M.E. Domine, L. Nemeth, S. Valencia, J. Am. Chem. Soc. 124 (2002) 3194.
[21] A. Corma, M.E. Domine, S. Valencia, J. Catal. 215 (2003) 294.
[22] S.H. Liu, S. Jaenicke, G.K. Chuah, J. Catal. 206 (2002) 321.
[23] Y. Zhu, G. Chuah, S. Jaenicke, J. Catal. 227 (2004) 1.
[24] Y. Zhu, S. Jaenicke, G.K. Chuah, J. Catal. 218 (2003) 396.
[25] D. Klomp, J.A. Peters, U. Hanefeld, in: J.G. De Vries, C.J. Elsevier (Eds.), Handbook of Homogeneous Hydrogenation, 3, Wiley-VCH, Weinheim, 2007, p. 585, Chapter 20.
[26] J.R. Ruiz, C. Jimenez-Sanchidrian, Curr. Org. Chem. 11 (2007) 1113.
[27] G.K. Chuah, S. Jaenicke, Y.Z. Zhu, S.H. Liu, Curr. Org. Chem. 10 (2006) 1639.
[28] S. Inagaki, S. Guan, Y. Fukushima, T. Ohsuna, O. Terasaki, J. Am. Chem. Soc. 121 (1999) 9611.
[29] T. Asefa, M.J. MacLachlan, N. Coombs, G.A. Ozin, Nature 402 (1999) 867.

[30] B.J. Melde, B.T. Holland, C.F. Blanford, A. Stein, Chem. Mater. 11 (1999) 3302.
[31] Q. Yang, J. Liu, J. Yang, M.P. Kapoor, S. Inagaki, C. Li, J. Catal. 228 (2004) 265.
[32] J. Liu, Q. Yang, M.P. Kapoor, N. Setoyama, S. Inagaki, J. Yang, L. Zhang, J. Phys. Chem. 109 (2005) 12250.
[33] K. Nakajima, I. Tomita, M. Hara, S. Hayashi, K. Domen, J.N. Kondo, Adv. Mater. 17 (2005) 1839.
[34] M.P. Kapoor, Y. Kasama, M. Yanagi, T. Yokohama, S. Inagaki, T. Shimada, H. Nanbu, L.R. Juneja, Microporous Mesoporous Mater. 101 (2007) 231.
[35] M.P. Kapoor, Y. Kasama, T. Yokohama, M. Yanagi, S. Inagaki, H. Nanbu, L.R. Juneja, J. Mater. Chem. 16 (2006) 4714.
[36] M.P. Kapoor, A. Bhaumik, S. Inagaki, K. Kuraoka, T. Yazawa, J. Mater. Chem. 12 (2002) 3078.
[37] M.P. Kapoor, A.K. Sinha, S. Seelan, S. Inagaki, S. Tsubota, H. Yoshida, M. Haruta, Chem. Commun. (2002) 2902.
[38] A. Bhaumik, M.P. Kapoor, S. Inagaki, Chem. Commun. (2003) 470.
[39] J.W. Akitt, R.H. Duncan, J. Magn. Reson. 15 (1974) 162.
[40] C.H. Lee, T.-S. Lin, C.-Y. Mou, J. Phys. Chem. B 107 (2003) 2543.
[41] S. Shylesh, A.P. Singh, J. Catal. 228 (2004) 333.
[42] D. Zhao, Q. Huo, J. Feng, B.F. Chmelka, G.D. Stucky, J. Am. Chem. Soc. 120 (1998) 6024.
[43] Y. Xia, R. Mokaya, J. Phys. Chem. B 110 (2006) 3889.
[44] R. Anwander, C. Palm, G. Gestberger, O. Groeger, E. Engelhardt, Chem. Commun. (1998) 1811.
[45] V.J. Shiner Jr., D. Wittaker, J. Am. Chem. Soc. 91 (1969) 394.
[46] S. Shylesh, R.K. Jha, A.P. Singh, Microporous Mesoporous Mater. 94 (2006) 364.
[47] C. Zapilko, Y. Liang, W. Nerdal, R. Anwander, Chem. Eur. J. 13 (2007) 3169.